19th IMEKO TC 4 Symposium and 17th IWADC Workshop
Advances in Instrumentation and Sensors Interoperability
July 18-19, 2013, Barcelona, Spain

Double Squirrel Cage Induction Motors: a New Approach to Detect Rotor Bar Failures

A. O. Di Tommaso, F. Filippetti*, Y. Gritli**, R. Miceli, C. Spataro

University of Palermo, Italy, sdeslab@unipa.it
**University of Bologna, Italy, fiorenzo.filippetti@unibo.it*
***National Institute of Applied Sciences and Technologies, Tunisia, yasser.gritli@esti.rnu.tn*

***Abstract*-** The paper deals with a diagnosis technique to detect rotor broken bar in double cage induction motor. The approach is based on the analysis of the motor vibration signals acquired by means of a piezoelectric accelerometer. In order to isolate and assess the contribution of the rotor fault components issued from vibration signals, the combined use of a frequency sliding and of a discrete wavelet transform analysis is proposed.
The approach is applicable not only under constant speed operating conditions, but also under time-varying conditions when the rotor fault components vary in the frequency spectrum. Moreover, the wavelet transform analysis of the vibrations can be extended to detect other failure modes of the induction motors.

I. Introduction

Various investigations on the different failure modes in induction motors have revealed that 19% of the overall motor faults are related to the rotor part [1]. In literature, the Motor Current Signature Analysis (MCSA) has been extensively used to detect rotor failures such as high-resistance connections in a rotor phase, mixed eccentricity and broken bars [2-6]. Nowadays diagnostic systems development [7-8] is more and more relevant in renewable energy integration [9-11] in the grid.
In this paper, we focus on double cage rotor motors which are typically used in those applications that require loaded and frequent starts, such as conveyors, crushers or compressors. Therefore, this category of motors is seriously subjected to fatigue failure of outer rotor cage due to the cyclic thermal/mechanical stress experienced. This is mainly due to the fact that the outer cage carries most of the current during the starting phases.
For double squirrel cage motors, as long as the contact impedance between the rotor bars and iron core is small or the copper bars are directly inserted into the laminated iron slots, the broken bars is no longer a physical condition ensuring an open circuit and inter bars or cross-path currents can flow [6]. Consequently, these currents interact with the radial component of the air-gap magnetic field, and compensate the rotor asymmetry caused by rotor bar breakage, which reduce the amplitudes of rotor fault components in stator currents. In this case, diagnosis technique based on MCSA to assess rotor conditions may fail, since the related components are too small to be detected.
In order to discern cases in which the presence of inter bars currents decreases the sensitivity of the MCSA, axial and radial vibrations analysis were investigated [12] and more recently, a combined use of current and vibration analysis was developed, by correlating the signal spectra to enhance broken bars detection ability under loaded and unloaded operating conditions of the motor [13]. However, the fault components, whose amplitudes must be monitored for diagnostic purposes, were mainly investigated in frequency domain using the classical Fourier analysis in order to track its evolutions.
The techniques based on Fourier analysis give satisfactory discrimination between healthy and faulty conditions, but it is applicable only under steady-state operating conditions and not under time-varying conditions. In fact, if the load is variable and/or the motor is fed by a variable-frequency converter, the rotor fault components vary in the frequency spectrum as a function of both mechanical and electrical frequencies, making difficult their detectability. In any case, to apply the Fourier analysis, it is necessary to accurately measure the speed of the motor, beside the motor supply frequency.
In this paper, after a brief description of the phenomenon which generates the rotor fault frequency components, the fault signatures issued from the axial core vibration signals are firstly investigated in frequency domain to evaluate the sensitivity of the fault components; then, a discrete wavelet transform (DWT) analysis is proposed to detect the fault. In this way, the time-frequency analysis allows to detect the fault without the need to accurately measure the speed of the rotor.

Experimental results, carried out in healthy and faulty motors, show that the proposed diagnosis technique not only can detect the existence of inter bar currents under broken bar failure, but also enhance the detectability of this type of fault.

II. Rotor fault frequency components

Like any other rotating electrical machine, the squirrel cage induction motor is subjected to both electromagnetic and mechanical forces symmetrically distributed.
In healthy conditions practically only the fundamental frequency f exists in stator currents. If the rotor is electrically damaged, the rotor symmetry of the machine can be lost and, in this case, a reverse rotating magnetic field related to an inverse sequence component of the rotor currents at frequency $-sf$ (s denotes the slip) appears. This inverse sequence is reflected on the stator side and produces the frequency component $(1-2s)f$. Consequently a torque ripple and a speed ripple are generated at frequency $2sf$, which modulates the amplitude of the rotating magnetic field [14].
This modulation produces two current components, i.e., an additional left-side component at $(1-2s)f$ and an additional right side component at $(1+2s)f$. Following this interaction process, the frequency content of the stator currents show series of fault components at the following frequencies $(1\pm 2ks)f$ (with k = 1,2,3,…), which decrease in amplitude as k increase. Since for double squirrel cage motors inter bars or cross-path currents can flow, these inter bar transverse currents interact with the radial stator flux density, generating axial forces.
These facts lead mainly to the presence of a first chain of fault frequency components at ($f_{mec}\pm 2ksf$) (with k = 1,2,3,…), and a second one at ((6-$2ks)f$) (with k = 1,2,3,…) in axial vibration directions (f_{mec} denotes the mechanical frequency of the rotor) [15].
Under healthy conditions, practically only the fundamental components at f_{mec} and at $6f$ exist in the vibration spectrum. Therefore, the detection of one of the above specified fault frequency component indicates that a rotor bar is damaged.
In a motor with broken rotor, the highest amplitude fault component that occurs in the axial vibration direction is f_{mec}-$2sf$ [16]. This component can be detected in the frequency domain by using a classic FFT. However, with this approach the diagnosis can become difficult for the following reasons:

1. the energy of this component depends on the motor load. The lower is the load, the less is the component amplitude;
2. the frequency of this component is a function of both the motor supply frequency and the motor speed;
3. when the load decreases, the slip decreases and the (f_{mec}-$2sf$) component becomes close the f_{mec} component.

To overcome these drawbacks it is necessary:

1. to acquire the signal with a very high signal to noise ratio;
2. to accurately measure both f_{mec} and f, which are variable parameters when the motor load is variable and/or the motor is fed by a variable-frequency drive;
3. to perform the FFT with a sufficiently long time window, in order to avoid the spectral leakage, making sure that, during the signal acquisition, the speed of the motor and the motor supply frequency are constant.

In order to limit some of the aforementioned problems, the usage of a discrete wavelet transform (DWT) is proposed.

III. The proposed approach

The principal feature of the DWT is its multiresolution analysis capability. In fact, by using the wavelet analysis the original discrete signal $S(n)$ is decomposed into various levels of approximation (a) and detail (d).
This can be implemented by a set of successive and complementary filter banks.
Using Nyquist sampling criterion, the outputs of the filters are then down sampled by factor 2, obtaining two signals a_1 and d_1 which represent respectively the approximation and the detail at the first level of decomposition. The same couple of filters are then applied to the a_1 signal, obtaining two signals a_2 and d_2 which represent respectively the approximation and the detail at the second level of decomposition. The procedure is repeated until the original signal is decomposed to a chosen level j of decomposition.
At the end of the iterations, the signal is represented by

$$S(n) = a_j(n) + d_j(n) + d_{j-1}(n) + \dots + d_3(n) + d_2(n) + d_1(n)$$

where the generic a_p signal covers the frequency range [0 - $f_B/(2^p)$] and the generic d_p signal covers the frequency range [$f_B/(2^p) - f_B/(2^{(p-1)})$], ($f_B$ is the bandwidth of the original signal $S(n)$ that in turn is equal to

ISBN-10: 84-616-5438-2 | ISBN-13: 978-84-616-5438-3

half of the sampling frequency f_C). Basically, by using the DWT, it is possible to obtain a time representation of various ranges of frequencies of the original signal.
To place the fault component (f_{mec}-$2sf$) in the chosen level of approximation, the axial vibration signal is shifted by modulating the signal with a sinusoid at a frequency equal to f_{mec}.
In such a way, all the information related to the broken bar fault is isolated and confined in a frequency band with range [0 - $f_B/(2^\wedge j)$], corresponding to the j level of approximation a_j. Then the shifted signal is analysed by means of DWT.
Actually, the same result could be simply obtained filtering the signal after the frequency shift. However, the use of the wavelet analysis is justified since, in other frequency bands, it is possible to localize fault components due to other failure modes of the motor.
Once the state of the machine has been qualitatively diagnosed, to obtain a quantitative evaluation of the fault degree, a multiresolution mean power indicator mPa_i at different resolution levels is introduced:

$$mPa_i = \frac{1}{N}\sum_{n=1}^{N}\left|a_i(n)\right|^2$$

where N is the number of samples and i is the level decomposition. In particular, given that the energy of the (f_{mec}-$2sf$) component is confined at the level a_J, mPa_j is adopted to quantify the extent of the broken bar fault.
Other frequency components, due to different failure modes, can be assessed in the same way.
In the next sections, frequency and time-frequency axial vibration analysis, under healthy and faulty conditions, are presented and commented.

IV. Experimental results

In this section experimental results issued from measured vibration signals are presented. To evaluate the fault detectability of the proposed approach, two identical double cage induction motors are available; one healthy, the second with a drilled bar near the end-ring (the bar was completely disconnected from the common end-ring). The characteristics of the double cage induction motors used in our experiments are the following: 5.5 kW rated power; 400 V rated stator voltage; 13 A rated current; 50 Hz rated frequency; 2870 rpm rated speed; 110 mm rotor diameter; 90 mm axial length of the rotor; 0.5 mm air gap length; 36 stator slots; 36 rotor slots.
A three-phase autotransformer of 30 kVA, 0-380 V is used as motor regulated supply. A four quadrants 7.83 kW DC electrical drive is adopted to reach the different planned load conditions. A piezoelectric accelerometer Brüel & Kjær, model 4507 B 005, for measuring axial vibrations of the core motors is mounted. A NEXUS 2693 model as a signal-conditioner is used. The signals have been acquired by a National Instrument PC-MIO-16XE-10 board inserted in a common PC.
In order to correctly understand the acquired data, the standard uncertainty of the whole measurement system was assessed [17 -18].
Considered the nearness of the inverter, an analysis of the electromagnetic immunity of the measurement system has been carried out [19-20].
The tests were carried out considering three load conditions; 100%, 50% and 25% of full load. In these conditions the slip is equal to 3 %, 1.3 % and 0.6 % respectively.

A. Frequency analysis

In order to detect the target fault component, various acquisitions of the axial vibration signals have been carried out, varying the sampling rate and the time window. In particular, figure 1 shows the spectra, issued from experimental tests for different load operating conditions, under healthy and faulty conditions. The vibration signals were acquired with a 3.2 kHz sampling rate and a 2 s time window.
The spectrums for the healthy machine are considered as reference in comparison to the faulty case. The magnitudes are normalized to the maximum amplitude of the harmonic component at frequency $6f$. Axial vibration signal spectra close to the mechanical frequency f_{mec} are depicted in figure 1 at (a) full load, (b) half load, and (c) quarter load under healthy (black) and faulty condition (blue).
As can be seen, with one rotor broken bar, the left side component (f_{mec}-$2sf$) significantly increases in comparison to the healthy case.
Particularly for the full load, the axial vibration spectrums depicted in figure 1-a, show a significant intensification of the fault component (*fmec-2sf*) for the motor with one rotor broken bar respect to the motor in healthy conditions. The same observation is true for half load condition (figure 2-b). However, to perform the diagnosis, the target component has to be localized in the frequency spectrum and, therefore, both the slip and the motor supply frequency must be accurately known.

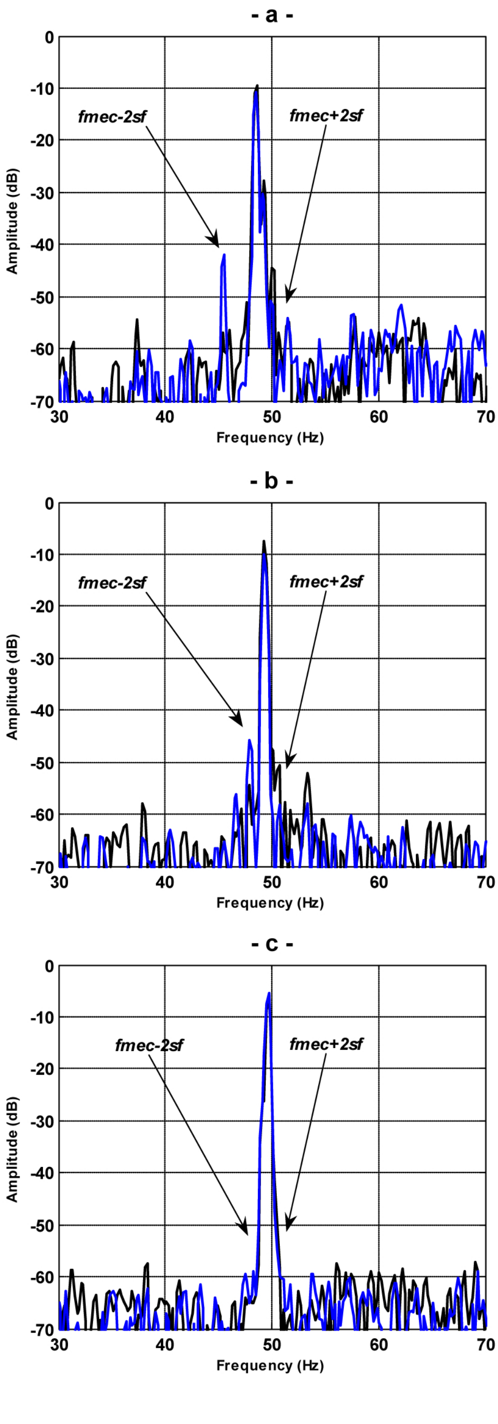

Figure 1. Axial vibration spectrums at (a) full load, (b) half load, and (c) quarter load operating conditions. Black line for healthy and blue line for faulty conditions.

For quarter or lower load levels, the fault component becomes close to f_{mec}, which complicates the fault detectability as depicted in figure 3-c. In this case, to detect the fault, the acquisition time window has been extended to 10 s, (i.e. acquiring 32000 sample), raising the frequency resolution to 0.1 Hz. However, in this case, both the motor speed and the motor supply frequency must be constant during the 10 s acquisition time window.

B. Time-frequency analysis

To perform the time-frequency analysis, in order to better compare the result with the ones obtained by using the frequency analysis, the same sampling rate has been used.
After the frequency sliding, performed modulating the axial vibration signals, the resulting signals were analysed by means of DWT.
With regard to the type of mother wavelet, a 10th order of Daubechies family was chosen, although other families were tested. With this wavelet family and sampling the signal at 3.2 kHz, the nine level of approximation a_9 represents the frequency band [0 – 3.125] Hz, where the fault component is always placed, at least for the considered load conditions.
All signals reported have been recorded for 5 s.
The wavelet decompositions of the axial vibration signals in healthy condition are used as reference in comparison to the faulty cases.
For full load operating conditions, axial vibration signals under healthy and faulty conditions are depicted in figures 2-a and 2-b respectively. The corresponding wavelet analysis results (the a_9 level of approximation), under healthy and faulty conditions are reported in figures 2-c and 2-d respectively. In healthy condition, the approximation signal of interest *(a_9)*, depicted in figure 2-c, do not show any variations. This indicates the absence of the fault component *(f_{mec}-2sf)*, leading to diagnose the healthy condition of the motor under full load operating conditions. For the same load operating conditions, large oscillations appear in the approximation signal a_9, depicted in figure 2-d.
The same observations are true for half load condition (figure 3), leading to a clear discrimination between healthy and faulty conditions, through the evolution of the wavelet signal a_9. For quarter (figure 4) load conditions, the fault components (*fmec-2sf)*, generate a very low, but still detectable contribution.
After the above qualitative analysis of the fault, a quantitative evaluation of the fault extend was conducted by using the mean power indicator mPa_9.
For the healthy motor mPa_9 is equal to 0.002 for the three load conditions; for the faulty motor, mPa_9 is equal to 0.092, 0.039 and 0.004 for full, half and quarter load respectively.
It is worth noting that to avoid ambiguous results, the motor must be enough loaded. Anyway, the developed approach is devoted to on-line diagnosis motors, which are mostly enough loaded (more than 50% of the rated load), making

the fault detection procedure more accurate.

The proposed diagnosis technique is also applicable when the rotor speed is not accurately known. In these cases, the vibration signals can be shifted by a frequency corresponding to the rotor speed mean value and the fault components, by applying the DWT, is isolated and confined in a frequency band with range [f_B /(2^j) - f_B /(2^(j-1))], corresponding to the j level of details d_j.

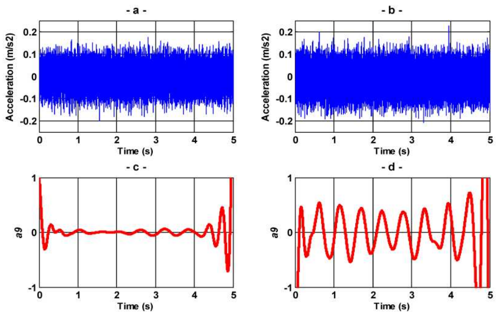

Figure 2. Axial vibration signals under (a) healthy, and (b) rotor broken bar conditions, and the corresponding DWT analysis (c) and (d) respectively, under full load conditions.

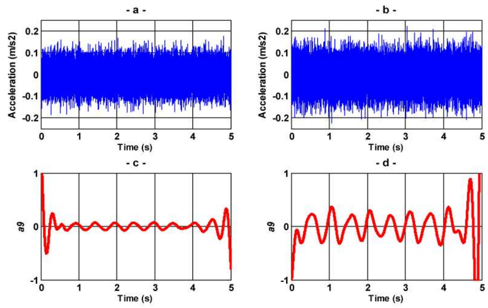

Figure 3. Axial vibration signals under (a) healthy, and (b) rotor broken bar conditions, and the corresponding DWT analysis (c) and (d) respectively, under half load conditions.

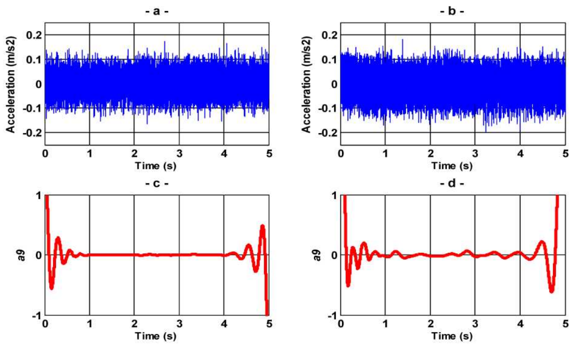

Figure 4. Axial vibration signals under (a) healthy, and (b) rotor broken bar conditions, and the corresponding DWT analysis (c) and (d) respectively, under quarter load conditions.

VI. Conclusions

For double squirrel cage motors, the diagnosis based on motor current signature analysis may fail due to the presence of inter bar currents, which reduce the amplitude of the tracked fault components in frequency domain. Vibration analysis may not only detect the existence of inter bar currents under broken bar failure, but also enhance the detectability of this type of fault by considering classical or advanced use of signal processing techniques. The analysis of the vibration signals in the time-frequency domain allows to overcome some drawbacks revealed in a simple frequency analysis. In particular the use of DWT lets detecting the faults, not only under steady-state operating conditions, but also when the motor speed and/or its supply frequency are variable. Our next target is the extension of the wavelet analysis to diagnose, classify and quantify other motor failure modes.

Acknowledgements

This work is partially funded by PON I-NEXT and by Uninetlab-Sdeslab of the University of Palermo.

References

[1] Bonnett, A.H., and Yung, C., "Increased Efficiency Versus Increased Reliability", *IEEE Industry Applications Magazine*, Vol. 14 No 1, 2008, pp. 29-36.

[2] Stefani, A., Yazidi, A., Rossi, C., Filippetti, F., Casadei, D. and Capolino, G. A., "Doubly Fed Induction Machines Diagnosis Based on Signature Analysis of Rotor Modulating Signals", *IEEE Transactions on Industry Applications*, Vol. 36 No 6, 2008, pp. 1717-1721.

[3] Wolbank, T.M., and Macheiner, P.E., "Modulation of transient reactances of induction machines caused by different types of eccentricity", *The IEEE International Symposium on Diagnostics for Electric Machines, Power Electronics and Drives* in Cracow, Poland, 2007, pp. 89-94.

[4] Gritli, Y., Di Tommaso, A.O., Miceli, R., Rossi, C., Filippetti, F., “Quantitative rotor broken bar evaluation in double squirrel cage induction machines under dynamic operating conditions”, *2013 8th International Conference and Exhibition on Ecological Vehicles and Renewable Energies* (EVER), Monte Carlo, Monaco, March 27-30 2013, DOI: 10.1109/EVER.2013.6521572, 2013, Page(s): 1 - 6.

[5] Gritli, Y., Di Tommaso, A.O., Filippetti, F., Miceli, R., Rossi, C., Chatti, A., “Investigation of motor current signature and vibration analysis for diagnosing rotor broken bars in double cage induction motors”, 2012 *International Symposium Power Electronics, Electrical Drives, Automation and Motion (SPEEDAM),* DOI: 10.1109/SPEEDAM.2012.6264465, 2012 ,Page(s): 1360 – 1365.

[6] Park, J., Kim, B., Yang, J., Lee, K., Lee, S.B., Wiedenbrug, E.J., Teska, M., and Han, S., "Evaluation of the Detectability of Broken Rotor Bars for Double Squirrel Cage Rotor Induction Motors", *the IEEE Energy Conversion Congress and Exposition*, Atlanta, Georgia, 2010, pp. 2493-2500.

[7] V. Cecconi, V. Di Dio, A. Di Tommaso, D. La Cascia, and R. Miceli, “Test Bench Realization and Application of Specific Working Cycles for the Characterization of Wheelchair Electrical Drives,” *in Industrial Electronics, 2006 IEEE International Symposium on*, 2006, vol. 3, pp. 2188–2193.

[8] V. Di Dio, R. Miceli, and G. Ricco Galluzzo, “Remote diagnosis and control of wheelchair electrical drive systems,” in Industrial Technology, 2004. *IEEE ICIT ’04. 2004 IEEE International Conference on*, 2004, vol. 2, p. 996 – 1001 Vol. 2.

[9] G. Cipriani, V. Di Dio, and G. Ricco Galluzzo, “A photovoltaic system suitable for the battery pack charging of an electrically power assisted velocipede,” *in Power Electronics, Electrical Drives, Automation and Motion (SPEEDAM)*, 2012 International Symposium on, 2012, pp. 1142–1147.

[10] R. Inguanta, S. Piazza, C. Sunseri, A. Cino, V. Di Dio, D. L. Cascia, R. Miceli, C. Rando, and G. Zizzo, “An electrochemical route towards the fabrication of nanostructured semiconductor solar cells,” *in Power Electronics Electrical Drives Automation and Motion (SPEEDAM*), 2010, pp. 1166–1171.

[11] V. Di Dio, D. La Cascia, R. Liga, and R. Miceli, “Integrated mathematical model of proton exchange membrane fuel cell stack (PEMFC) with automotive synchronous electrical power drive,” *in Electrical Machines, 2008. ICEM 2008. 18th International Conference on*, 2008, pp. 1–6.

[12] Concari, C., Franceschini, G., and Tassoni, C.," Differential Diagnosis Based on Multivariable Monitoring to Assess Induction Machine Rotor Conditions", *IEEE Transactions on Industrial Electronics*, Vol. 55 No. 12, 2008, pp. 4156-4166.

[13] Rangel-Magdaleno, J. J., Romero-Troncoso, R. J., Osornio-Rios, R. A., Cabal-Yepez, E., and Contreras-Medina, L. M., "Novel Methodology for Online Half-Broken-Bar Detection on Induction Motors", IEEE Transactions on Instrumentation and Measurement, Vol. 58 No. 5, 2009, pp. 1690-1698.

[14] Bellini, A., Filippetti, F., Tassoni, C., and Capolino, G. A., "Advances in diagnostic Techniques for induction machines", *IEEE Transactions on Industrial Electronics*, Vol. 55 No 12, 2008, pp. 4109-4126.

[15] Walliser, R.F., and Landy, C.F., "Assessment of interbar currents in double cage induction motors with broken bars ", *IEEE Transactions on Energy Conversion*, Vol. 9 No. 1, 1994, pp.159-164.

[16] Di Tommaso, A.O., Miceli, R., and Ricco Galluzzo, G., "Monitoring and Diagnosis of Failures in Squirrel-Cage Induction Motors Due to Cracked or Broken Bar", *the IEEE International Symposium on Diagnostics for Electric Machines, Power Electronics and Drives* in Bologna, Italy, 2011, pp. 39-44.

[17] C. Spataro: “A/D Conversion Based Measurements: Identification of the Parameters for the Uncertainty Evaluation”, *Proc. of AMUEM 2009 – International Workshop on Advanced Methods for Uncertainty Estimation in Measurement* - Bucurest, Romania, 07-08 July 2009.

[18] C. Spataro: “ADC Based Measurements: a Common Basis for the Uncertainty Estimation”, *Proc. of 17th IMEKO - TC4 Symposium*. Kosice, Slovakia. September, 08-10. 2010

[19] S. Nuccio, C. Spataro, G. Tinè: “Electromagnetic immunity of a portable PC-based measurement instrument”, Proc. of IWADC 2003, Perugia, Italy, September 2003.

[20] S. Nuccio, C. Spataro, G. Tinè: “Virtual instruments: Uncertainty evaluation in the presence of unknown electromagnetic interferences”, Proc. of AMUEM 2008 – *International Workshop on Advanced Methods for Uncertainty Estimation in Measurement* - Trento, Italy, 21-22 July 2008, pp. 56-61.